World Conference on
Timber Engineering
Oslo 2023

NUMERICAL SIMULATION OF FIRES WITH EXPOSED TIMBER

Sabrina Spörri [1], Chamith Karannagodage [2], Joachim Schmid[3], Andrea Frangi [4]

ABSTRACT:

The burning of timber is a complex process because of its inhomogeneous structure and the interlinked processes of material decomposition and gas-phase combustion. One approach to predict the burning behaviour of timber in fire is through simulations. This work studies the charring properties of the timber with the complex pyrolysis model in the Fire Dynamic Simulator (FDS). A timber specimen of 260 mm × 225 mm × 120 mm exposed to an external heat flux in a non-standard experimental environment has been simulated with the FDS using the appropriate input parameters for the pyrolysis and gas phase combustion. The simulations also investigated the influence of the moisture and temperature-dependent specific heat on the simulation results. When the simulation results were compared to the experimental results, there was a good agreement for the charring rates, with a maximum deviation of 0.06 mm/min. The results showed the importance of moisture in the pyrolysis model to obtain accurate results. The findings suggest that the FDS can be used to study and predict the char depth of timber to calculate the residual cross-section for building designs.

KEYWORDS: Fire dynamics, Numerical simulations, Exposed timber, Timber pyrolysis

1 INTRODUCTION

Fires are a dynamic process with their intensities being dependent on the prevalent boundary conditions. An important factor influencing the behaviour of fires is whether the fire is burning openly or enclosed in a compartment. In open fires, there is an unlimited supply of oxygen for the combustion reaction and the resultant smoke plume can rise unimpeded depending on the stability of the atmosphere. In contrast, when a fire occurs in a compartment, the oxygen supply to the combustion reaction is limited by the size of the opening(s) and the smoke plume is trapped within the enclosure. In these types of fires, all the enclosing components are heated up in a fire, especially in the upper part of the compartment, where the hot combustion products are trapped beneath the ceiling and form a hot layer.

The flames above the fire, the heated surfaces of enclosing components, and the layer of hot combustion products accumulated under the ceiling can all be considered sources of radiant heat flux. These radiating sources potentially contribute to further heating the burning and non-burning fuel. To summarise, the main aspects influencing the compartment fire dynamics are the distribution and the type of fuel load, the compartment geometry, the ventilation configuration and the material of the compartment boundaries [1].

Nowadays, the traditional construction material timber is experiencing a renaissance as it is an environmentally-friendly material which contributes to a sustainable construction, but also satisfies the architectural need for new designs and aesthetics [2–4]. When the boundary surfaces consist of combustible material like timber, this will significantly impact the compartment fire dynamics by adding an additional fuel load to the fire. Studies have shown that the additional fuel will increase the severity of the external flaming and the thermal load that must be resisted by the structure to ensure that safety criteria are satisfied [5,6].

Recent trends have increased the market demand for the larger floor spaces (fire compartments), increased quantities of visible (unprotected) timber and taller buildings. These trends will not only influence the duration and the intensity of the compartment fires but also the techniques used to fight them [7]. Very recent changes in regulations in UK and Scandinavia require the determination of “physically based design fires”. These design fires must consider the compartment geometry, architectural linings and the potential influence of any combustible structures (timber).

Although proposals for modifying the parametric fire design are available [7], it appears to be challenging to

[1] Sabrina Spörri, ETH Zurich (IMFSE), Switzerland, sabrina.spoerri@gmx.ch
[2] Chamith Karannagodage, ETH Zurich, Switzerland, karannagodage@ibk.baug.ethz.ch
[3] Joachim Schmid, ETH Zurich, Switzerland, schmid@ibk.baug.ethz.ch
[4] Andrea Frangi, ETH Zurich, Switzerland, frangi@ibk.baug.ethz.ch

https://doi.org/10.52202/069179-0231

describe the complex aspects of the fire dynamics in timber structures with the available design frameworks. Consequently, it is expected that a performance-based design allows a greater design flexibility, promoting innovation and a better use of resources allowing for a better fire risk management [8]. When applying a performance-based approach to timber structures, a key input that is missing is the development and the combustion of the char layer in the compartment environment.

Moreover, reliable numerical models could decrease the necessity of full-scale tests, which are costly and require a large amount of resources. That way, fire-design approaches could rely on numerical models to assess the use of innovative and more sustainable building materials and allow maximum freedom in building design while upholding the required level of building safety.

This paper simulates the burning behaviour of a timber specimen using a field model. This simulator couples the gas and solid phase processes that occur in a fire. The gas phase processes are the combustion of flammable gases and the local air flow whilst the solid phase processes include the thermal degradation of fuel (pyrolysis). A summary of the simulating steps and an overview of the most important parameters for the simulations are presented with the comparison of results from the fire experiment.

2 STATE OF THE ART

2.1 BURNING PROCESS OF TIMBER

Timber is a substance with an anisotropic structure [8] and mainly constitute with the cellulose, hemicellulose and lignin [10]. Depending on the wood species, the percentage of these three molecules vary, but a rough approximation for dry wood is 50% of cellulose, 25% of hemicellulose and 25% of lignin [10]. Timber naturally contains moisture. This can exist either as bound water in the cell walls (hygroscopic water) or as free water in the voids of the wood (capillary water) [13].

The burning process of timber can be divided into two main processes. First, when the timber is exposed to heat, at high temperatures it begins to change its cellular structure initiating the pyrolysis process. Pyrolysis is the thermal decomposition of fuel material [14]. At elevated temperatures, timber degrade the constituent natural polymers producing volatile gases, tar and char. Secondly, when the pyrolysis volatile gases mix with ambient air it makes a combustible mixture which can lead to a flaming combustion (fuel oxidation) [15].

2.1.1 Pyrolysis of timber

Timber shows different stages in the pyrolysis process due to its material properties as shown in Figure 1. When heated to 100°C, the moisture within the timber starts to evaporate. Upon further heating, the pyrolysis process begins when the fuel reaches around 200°C producing volatiles. This is initially a relatively slow process until the fuel reaches 300°C after which the production rate of the volatile gases increases. [15].

On a general level, the pyrolysis is an endothermic reaction, and the energy is needed to break the polymers into smaller parts to present in the gaseous phase [12,15]. This process produces inert and combustible gases, liquid tar, solid carbon-rich non-volatile char and inorganic non-burning ashes as shown in Equation (1) [15].

$$wood \rightarrow gases + tar + char + ash \quad (1)$$

The produced gases are mainly CO, CO_2 and H_2O. The combustible gases will further undergo the combustion as explained in the Section 2.1.2. The char contains heavier and larger molecules which stay on the timber surface forming a layer which affects the heat transfer to the virgin timber. The char can further undergo the solid phase oxidation which is visible as smouldering or glowing combustion. This decomposition also creates a surface regression of the timber and makes the cross-section smaller [4]. The char yield of the reaction is influenced by the presence of organic impurities in the wood and for most of the situations, the char formation starts around 300°C [15]. It should be noted that, this is a simplified description of the processes. In reality, several interdependent chemical reactions occur at the same time and the process is further complicated by the inhomogeneity of wood and the influence of the produced char layer [9].

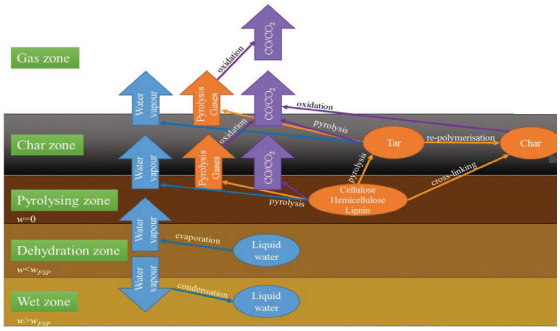

Figure 1: *Chemical and physical processes of a burning timber specimen. Modified from [15].*

2.1.2 Gas phase combustion

The mixing of combustible pyrolysis products with air in the right proportion (flammability limit) and in the right environmental conditions leads to their oxidation. This process is called the gas phase combustion [12,15]. This is an exothermic process producing the energy which could further enhance the production of the pyrolysis gases by transferring heat to the surface of the fuel [15]. If this heat feedback mechanism produces enough heat to release further volatiles within the flammability limit, then the mixture can sustain flaming combustion. The flammability limit or the flammable limit is the amount of combustible gas in an air mixture when the mixture is flammable.

https://doi.org/10.52202/069179-0231

2.2 PYROLYSIS MODELS

As the overall process of pyrolysis is very complex to work with, a lot of models have been proposed to describe the pyrolysis process in a simplified way adapting to desired real-life applications. Moghtaderi [13] gives an overview of the different pyrolysis models and classifies them based on their decomposition reaction as how the conversion from the virgin fuel into the gaseous products and char residues is described.

Distinctions are to be made between simple thermal models and comprehensive models. These two groups differ in the way they define the conversion of the fuel into the products, by the pyrolysis rate. The simplified models derive the rate only from the energy balance and the comprehensive models by a combination of kinetic schemes, mass and energy balances [13].

2.2.1 Simple thermal models

Simple thermal models use the criteria of a critical pyrolysis temperature while ignoring the physical and chemical processes to derive the pyrolysis rate (i.e., mass loss rate) from the energy balance. Depending on the solution method used to solve the equation, the simple thermal models are divided into the Algebraic, Analytical and Integral models. Equation (2) shows an example of an analytical simple thermal modal where the mass loss rate is proportional to the net absorbed heat flux for a thermally thin slab exposed to constant heat flux [13],

$$\dot{m} = \frac{\dot{q}_e^{''} A_s}{\dot{Q}_p} \tag{2}$$

where $\dot{m}$ = Mass loss rate [kg/s], $\dot{q}_e^{''}$ = External heat flux [kW/m^2], A_s = Surface area of solid [m^2], $\dot{Q}_p$ = Heat of pyrolysis [kJ/kg]

These models have the advantage of being relatively simple to use. However, they have the disadvantage of relying on a critical temperature for the ignition and neglecting many chemical processes. The use of a critical temperature simplifies the fact that the chemical processes occur faster than the diffusion processes. This is only true in very high temperatures. However, the chemical kinetics play a big part at the lower temperatures.

2.2.2 Comprehensive models

The comprehensive models incorporate the chemical and diffusion processes that occur during the pyrolysis. They have thus overcome the fundamental nature of a simple thermal model. As a result, these comprehensive models can also include the thermal degradation processes. Furthermore, other processes like heat transfer, morphological changes, expansion, shrinkage, char formation, chemical reactions, and in-depth radiation are also frequently included in the models [16]. The examples of the comprehensive models are Gypro, ThermaKin, Pyropolis, and FiresCones [16]. Because of the complexity of these models, numerical solution methods such as finite difference or finite volume are almost always required to solve the equations.

The comprehensive models are classified as follows by the reaction scheme,

- One-step global reaction schemes
- One-step multi-reaction schemes
- Multi-step semi-global schemes

The simplest one is the one-step global reaction scheme which only considers a primary reaction like the conversion of virgin timber into products as given in Equation (1). In this model, the thermal degradation products are considered as lumped materials. The pyrolysis rate is calculated by the Arrhenius expression given in Equation (5), which is proportional either to the weight residue or the weight loss of the fuel [13]. The input parameters for the equation need to be defined experimentally.

The one-step multi-reaction scheme is a more detailed reaction scheme than the previous one. Here also, each component undergoes only one independent reaction, but this time the timber is not modelled as a lumped material but made out of several components. Each of these components goes through a different reaction that occurs in parallel. In this case, the pyrolysis rate is the sum of the reaction rates of each component weighted by the percentage of each component. The subsequent reaction that some of these products can undergo is the next step in the complexity. These are known as the secondary reactions [10], and one example is the char oxidation. Multi-step semi-global schemes are the models that take such reactions into account.

Some comprehensive models can also consider the effect of moisture presence in the pyrolysis process. However, a disadvantage of these comprehensive models is that many input parameters are needed even with a simple reaction scheme. That number increases drastically if more complex reaction schemes are used.

2.3 FDS PYROLYSIS MODEL

The Fire Dynamics Simulator (FDS) developed by the National Institute of Standards and Technology (NIST) is a Computational Fluid Dynamics (CFD) software package which solves simplified forms of Navier-Stokes equations numerically. The FDS can be used to simulate low-speed thermally driven fluid flow with the smoke plume. FDS is a powerful tool to predict heat generation and transfer from a fire [17]. The main models in FDS are hydrodynamic, combustion, and radiation transport models [18].

The combustion model is mainly used as a single-step, mixing-controlled chemical reaction. The combustion reaction includes air, fuel and products which are treated as lumped species and explicitly tracked in the simulations.

2.3.1 Pyrolysis model

FDS has the option to include different types of pyrolysis models, ranging from simple thermal ones to complex models based on the kinetics [18,19]. This study will use

the complex pyrolysis model from FDS. The complex pyrolysis model needs to define one or several chemical decomposition reactions and input data to calculate the reaction rate as explained in the previous section. The FDS definition of the pyrolysis reaction rate $r_{\alpha\beta}$ is a combination of solid and gas phase conditions and defines the reaction rate depending on the temperature of the solid T_s. The definition in the FDS contains the following sub-terms, Equations (3)–(5) [19]. In this study, only the reactant dependency and the Arrhenius function were used to define the reaction rate.

$$r_{\alpha\beta} = Reactant\ dependency \times Arrhenius\ function \times Oxidation\ function \times Power\ function \quad (3)$$

$$Reactant\ dependency = \left(\frac{\rho_{s,\alpha}}{\rho_{s(0)}}\right)^{n_{s,\alpha\beta}} \quad (4)$$

$$Arrhenius\ function = A_{\alpha\beta} exp\left(-\frac{E_{\alpha\beta}}{RT_s}\right) \quad (5)$$

where α = Material component in material layer, β = Name of reaction, $\rho_{s,\alpha}$ = Solid density of material component α [kg/m^3], $\rho_{s(0)}$ = Initial solid density of material layer [kg/m^3], $n_{s,\alpha\beta}$ = Partial reaction order for material component α in material layer and reaction β, $A_{\alpha\beta}$ Pre-exponential factor [1/s], $E_{\alpha\beta}$ = Activation energy [J/mol], R = Gas constant [J/K·mol], T_s = Temperature of solid [K]

Furthermore, the heat transport through the depth of the solid is calculated by the conduction in FDS. In this study, the heat conduction is only considered as one-dimensional into the solid.

2.3.2 Gas combustion model

The gas combustion model is a single-step mixing controlled combustion based on the Eddy Dissipation Concept where the mixing is approximated as having been burnt [19] and where only one fuel can react [18]. The chemistry model relies on a reaction of the following form as in Equation (6).

$$C_xH_yO_zN_v + v_{O_2}O_2 \rightarrow v_{cO_2}CO_2 + v_{H_2}H_2O + v_{co}CO + v_sSoot + v_{N_2}N_2 \quad (6)$$

Therefore, the user needs to specify the chemical equation of the burning fuel along with the yield of CO, soot and the volume fraction of the hydrogen in the soot. The enthalpy of formation of the gaseous fuel can either be specified directly for each gas or can be calculated from the (specific) heat of combustion of the reaction if the enthalpy of formations of all the other molecules in the reactions are known [19]. This second approach will be chosen in this study for the definition of the enthalpy of formation.

3 PYROLYSIS MODELLING WITH TIMBER IN FDS

3.1 INPUT PARAMETERS FOR THE FDS PYROLYSIS MODEL

The pyrolysis model used in this study was a one-dimensional heat transfer model with a simple, one-step global reaction scheme. To be compatible with the experimental data described in the section 3.4 "Experiment description", spruce was selected as the wood type. As shown in Equation (7), the chemical reaction was defined as the conversion of spruce into char and pyrolyzate.

$$Spruce \rightarrow char + pyrolyzate \quad (7)$$

In the experimental setup, the spruce sample had a moisture content of 12%. However, the simulations were started with dry spruce to keep the reaction scheme simple. Subsequently, the moisture content was added to the simulation. Only the reactant dependency and the Arrhenius function are used to calculate the reaction rate (Equations (3)–(5)). The oxidation function and power function of the FDS pyrolysis model were not studied further during this study. The default FDS values were used for those terms in the analyses.

For estimating the material and kinetic properties of spruce and char, the values were based on the research of Rinta-Paavola and Hostikka [20]. Thermogravimetric analysis (TGA) was used in the aforementioned study to estimate the yield of char and pyrolyzate, as well as the activation energy and pre-exponential factor [20]. This work provided the input parameters for the pyrolysis of spruce for simple and parallel reaction scheme in FDS. Further, these input parameters were validated and optimised against the cone calorimeter experiments at different heat fluxes. The value for the heat of combustion was derived from the micro-combustion calorimetry (MCC) experiments [20].

The heat of combustion is the effective heat of combustion, which is also the default definition in the FDS [18]. The heat of reaction for this simple reaction is defined as endothermic and is the optimised value by model fitting for a heat flux of 35 kW/m^2 in a cone calorimeter test [20]. Table 1 summarises the input parameters that were used for the decomposition process in the FDS simulation.

Table 1: *Input parameter for decomposition process [18,20]*

Parameter	Value
Number of reactions	1
Yield of char	0.16
Yield of pyrolyzate	0.84
Activation energy (J/mol)	190'500.00
Pre-exponential factor (1/s)	4.691×10^{13}
Absorptivity (1/m)	50'000.00
Reaction order	1
Heat of combustion (kJ/kg)	14'000.00
Heat of reaction (kJ/kg)	19

https://doi.org/10.52202/069179-0231

Other material properties for spruce, char, and pyrolyzate should be defined in addition to the pyrolysis parameters. These parameters for the two materials are shown in the Table 2 and in the text following the table. The next section will provide the information on the gaseous product "pyrolyzate".

Table 2: *Material properties for spruce and char [20,21]*

Parameter	Spruce	Char
Density (kg/m^3)	408	59
Emissivity (-)	0.9	0.85
Conductivity (W/m K)	0.09	0.22

The conductivity for spruce was the optimised value by model fitting for a heat flux of 35 kW/m^2 in a cone calorimeter test. The char density of 59 kg/m^3 was in the same range as reported in the literature, where the initial char density is 10–20% of that of the dry wood [22]. The value for the emissivity of char was from Chaos [21].

The last input parameter needed is the specific heat for spruce and char. They were defined as temperature-dependent in the publication of Rinta-Paavola and Hostikka [23]. The specific heat capacity of spruce ($C_{p,spruce}$) was defined as a linear growth from 30°C with 920 J/(kg·K) to 230°C with 1800 J/(kg·K). The specific heat capacity was assumed to be constant below and above that temperature. The specific heat of char ($C_{p,char}$) was defined by Equation (8).

$$C_{p,char} = 1430 + 0.355 \cdot T - \frac{7.32 \times 10^7}{T^2} \qquad (8)$$

where T = Temperature [K]

3.2 INPUT PARAMETERS FOR THE FDS GAS COMBUSTION MODEL

The main fuel for the gas combustion is the gaseous product pyrolyzate produced by the decomposition reaction in Equation (1). The input parameters for the gas combustion in the FDS were defined as follows; the chemical composition of the burning gas of spruce (C:1, H:3.584, O:1.55, N:0), the soot yield (0.015), the effective heat of combustion (14 MJ/kg), the viscosity (0.00059 kg/m·s) and the diffusivity (4.3×10^{-7} m^2/s) [20],[23][24].

For the conductivity, the value for the spruce was used [20], the diffusivity was the axial diffusivity for dry ash [23] and the viscosity was for wood [24]. For the surrogate molecule of the thermal radiation, FDS has a predefined list to choose from [18]. From there, a chemically similar molecule to the gaseous product was chosen, which was 'METHANOL'. Additionally, the default FDS values were used for the other parameters in the gas combustion model.

3.3 ANALYSING METHOD TO DETERMINE THE CHARRING DEPTH AND CHARRING RATE

The temperature profile inside the timber specimen was used to calculate the position of the charring front in the simulations. It was defined as the 300°C isotherm [25]. The distance from the surface of the timber specimen to the position of the charring front at the end of the simulation was then defined as the charring depth. The charring rate was calculated by dividing the charring depth by the simulation time when the charring front reached that depth. An experimental setup was followed to create the simulation environment to model the timber pyrolysis and to evaluate the performance of the simulation.

3.4 EXPERIMENT DESCRIPTION

The Fire Apparatus for Non-standard Heating and Charring Investigation (FANCI) [4] was chosen as the experimental setup. It enables the investigation of the charring behaviour, the char layer surface regression, and the temperature distribution in a timber specimen, among other things. The experimental environment is called non-standard as the application of an airflow from 1 to 6 m/s is possible with a variable incident heat flux up to 120 kW/m^2 from a quick response heat panel to ignite the specimen [4]. Figure 2 and Figure 3 show the experimental setup used for the fire apparatus.

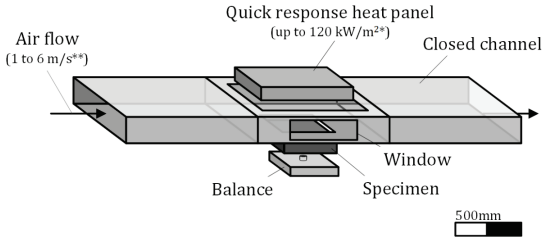

* variable external heat flux

** reference velocity at normal temperature

Figure 2: *Schematic view of the FANCI experiment setup [4]*

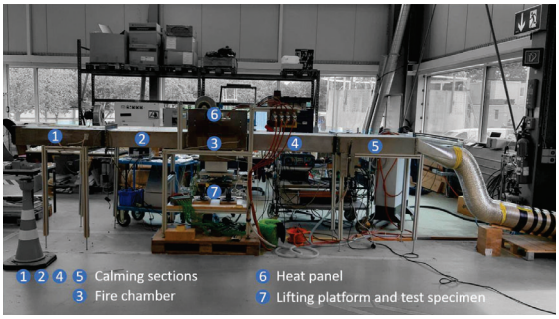

Figure 3: *FANCI test setup with the different components [27]*

The apparatus consisted of a long tunnel made of five sections, each section with a length of approximately 0.9 m, a width of 0.5 m and a height of 0.15 m as shown in Figure 3 [27]. The total length was approximately 4.5 m. Steel plates with a thickness of 1.5–3.0 mm were used to make these sections. The airflow was from the left

to right with respect to Figure 2. The timber specimen was placed in the section 3, called the fire chamber and positioned on the floor opposite a heat panel on the ceiling. The specimen had a length of 260 mm, a width of 225 mm and a thickness of 120 mm. The wood type was spruce, with a moisture content of around 12%.

For the comparison with the simulation results, the test JF00 from the FANCI test series was chosen [26]. In this experiment, a timber specimen was placed in the apparatus at a prevailing velocity of around 2.5 m/s, and the heat flux panel was calibrated to produce an incident heat flux of 96.4 kW/m^2 on the surface of the timber specimen. The specimen was heated by the heat panel for 20.1 min. The ignition occurred after ca. 0.42 min. The reported charring depth was 24 mm which was reached after 20 min. The charring rate for this test was 1.21 mm/min and the surface recession was 0.22 min/mm.

3.5 FDS MODEL

3.5.1 Geometry and mesh

The length of the tunnel for the simulation was shortened to 2.2 m instead of the length of 4.5 m in the actual experiment to reduce the computational time during the simulations. This was chosen after a sensitivity analysis to investigate the influence of the mesh size (1.25 cm, 1.0 cm and 0.625 cm) and the tunnel length on the airflow. Following the mesh sensitivity analysis, a mesh size of 1 cm was selected for the simulation. As there were no significant differences in the flow fields between the two geometries for all the simulations, a shortened geometry of the FANCI tunnel appears to be reasonable and capable of incorporating all the measurements that were measured in the FANCI-test experimental setup. The Figure 4 compares the geometry of the experiment and the simulation.

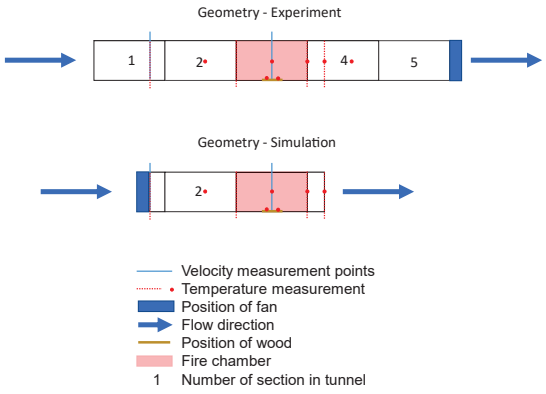

Figure 4: *Comparison of the geometry of the experiment and the simulation*

3.5.2 Temperature measurement

Following the experimental setup, gas temperature values were measured on the centre line of the tunnel. In the simulation, the temperature devices were distributed between the start of the fire chamber and the outlet, as shown in the Figure 4. Similar to the experimental setup, additional temperature measurements were done on the surface of the timber specimen and inside the solid.

3.5.3 Implementation of the mesh inside the timber specimen

For further analysis of the properties inside a solid, FDS has a special output recording option called &PROF [18]. This provides in-depth profiles of physical properties such as inlaid temperature, overall density, or density of different solid material components. The spacing of the solid grid defines the recording positions of these properties, which is done automatically by FDS unless changed manually [18].

Equation (9) defines the size of a solid phase cell or, in the case of one-dimensional heat transfer, the thickness of one layer inside the solid in the FDS. The simulation thickness is less than or equal to the calculated value.

$$\sqrt{\frac{\tau k}{\rho c}} \tag{9}$$

where τ = time constant [s], k = thermal conductivity [W/m·K], ρ = density [kg/m^3] and c = specific heat [J/kg·K].

By default, the distance between layers is smaller at the solid's surfaces and increases towards the middle by doubling their size to reduce the computational resources. They begin to shrink again as they approach the mid-depth. To some extent, the user can modify this solid grid by making the node spacing more uniform or by changing the mesh cells. The code line STRETCH_FACTOR, which is set to 2 by default, is responsible for the non-uniform spacing. This STRETCH_FACTOR was set to 1.0 for all the simulations to achieve a uniform spacing after a solid mesh sensitivity analysis. This resulted in approximately 248 layers inside the solid with a maximum thickness of 0.5 mm.

It should be noted that the spacing in Equation (9) is dependent on the thermal properties of the materials. when one of these changes, the number of layers also changes. Furthermore, if the burning causes the material to shrink or swell, resulting in a change in material thickness, FDS rechecks the total number of layers and adds or removes the layers as necessary.

3.6 OVERVIEW OF THE SIMULATIONS

The information available from the experiment for heating the timber specimen was an estimate of the incident heat flux on the surface of the timber specimen. Two heating methods were tested to achieve a similar incident heat flux on the timber surface in the FDS simulations.

The first option involved simulating an external heat flux with the same intensity as the experimental incident heat flux over the timber specimen. This simulation is named "S1-exHF" in this paper. In this method, the heat flux functions similarly to a perfect radiant panel or conical heating unit [18]. Option two involved defining a heat

https://doi.org/10.52202/069179-0231

panel on the tunnel ceiling above the wood specimen and calibrating it so that the amount of incident heat flux measured on the timber specimen surface has the same intensity as the one estimated in the experiment. This simulation is named "S2-HP". Dry timber specimens were simulated in these simulations using the temperature-dependent specific heat and the other input parameters listed in Section 3.1 and considered as the "standard simulations".

Additional simulations with modified input parameters were run apart from the standard simulations. One modification was introducing the moisture content to the timber specimen into the standard simulations ("S1-exHF-moisture" & "S2-HP-moisture"). This change also agrees with the experimental information, where the spruce had a moisture content of 12%. The goal was to see whether a more complicated pyrolysis model adds additional value to the output.

The other modification was to see the influence of the temperature-dependent input parameters on the simulation results. Instead of a temperature-dependent parameter, constant values were used for the specific heat of spruce and char in the standard simulation. This simulation is called "S1-exHF-cp". The simulation time was similar to the duration of the experiment, which was 20.1 (min).

4 RESULTS

4.1 COMPARISON OF THE IGNITION METHOD

The two methods which were used to ignite the timber specimen, once by a constant external heat flux over the specimen ("S1-exHF") and once by a heat panel ("S2-HP") showed similar results as shown in the Figure 5. The surface temperature measurements are slightly higher for the heat panel than the heat flux.

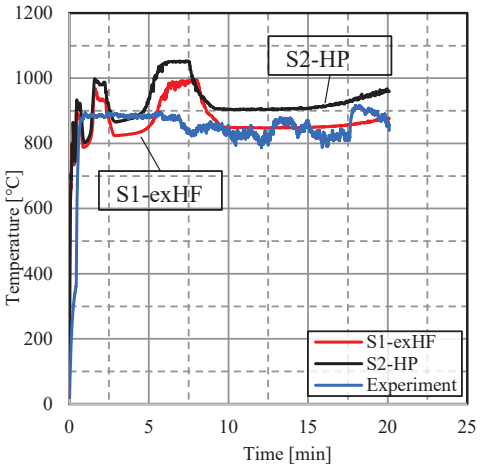

Figure 5: *Comparison of the surface temperature for experimental and modelling results for two ignition methods (S1, S2)*

The comparison of the mean surface temperatures shows temperature measurements of simulation to be very close to the experimental measurements but slightly higher. Taking into account that the measurements in the simulation were done by direct temperature measurements where the higher measurements were expected than those in the experiment where thermocouples have been used with a thermal inertia. Overall, it is visible that the temperature measurements in the simulation are in a good range. The external heat flux over the specimen is the best method to simulate the incidence heat flux on the specimen to compare with the experiment.

4.2 SURFACE TEMPERATURE MEASUREMENTS

The Figure 6 shows the comparison of the surface temperature of the specimen for different simulations compared to the experimental temperature values. The mean surface temperature for the experiment was 834.7°C, and the simulation values for the standard case and modified simulations are within 5% of this experimental mean value. These findings show that the surface temperatures in the experiment and simulations were very similar, indicating that the simulations had a similar fire exposure to the experiment. The modifications to the standard cases in the simulations have no significant effect on the results when compared to the experimental values.

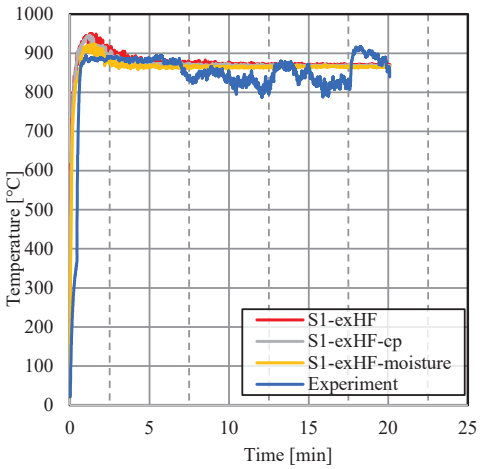

Figure 6: *Comparison of the surface temperature for experimental and modelling results for three specimens: dry, with constant specific heat and moist*

4.3 INLAID TEMPERATURE MEASUREMENTS

The temperatures inside the timber specimen from the experimental data are compared with the simulated results at various depths in the Figure 8. The thermocouple positions correspond to the depths measured in the experiment from the exposed surface as shown in the Figure 8.

Overall, the comparison indicates that the simulation temperatures are generally higher than the experiment. The above-mentioned trend was observed throughout the entire time, particularly at the deeper depths from the exposed surface. On the other hand, at the 6 mm and the

https://doi.org/10.52202/069179-0231

12 mm, the simulation temperatures close to the exposed surface are higher at the beginning of the test, but the experimental values gradually increase and become higher than the simulation values during the tests, as shown in the Figure 8. Further, at a depth of 18 mm, the simulation and experimental results end up in a similar temperature range. The comparison of the experimental and simulation results with ignition by a heat panel revealed the same pattern.

The reasons for the above difference could be diverse and might be related to the simplified definition of the charring process in the simulation or due to the inertia of the thermocouples in the experiment. Furthermore, the reaction parameters that were given as an input need to be optimised to define a realistic heat transfer into the solid for a non-standard fire exposure.

4.4 CHAR PROPERTIES

The graph in the Figure 7 compares the progression of the charring front through the timber specimen using the 300°C isotherm profile, where timber might char for the three simulations where the ignition was simulated by an external heat flux and for the experimental data. The charring rate has calculated using a linear regression in the experimental analysis. The data points in the simulations, on the other hand, show a logarithmic behaviour for the progression of the 300°C isotherm.

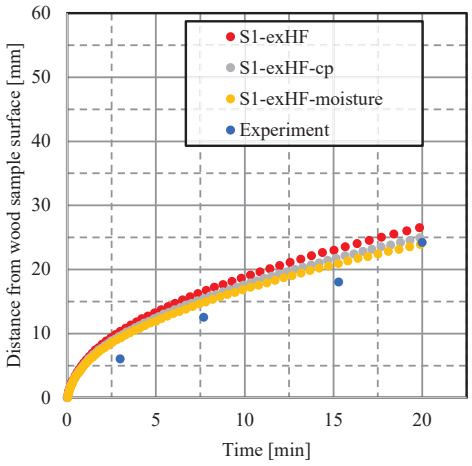

Figure 7: *Comparison of the char layer progression for experimental and modelling results for three specimens: dry, with constant specific heat and moist*

The Table 3 presents the charring depth and calculated charring rates for the simulations and the experiment at the end of the test. The comparison shows higher charring rates for the simulations with the dry specimen. The maximum difference in the charring rate for the simulations with the dry specimen is a 15.7% deviation from the experimental charring rate. On the other hand, the results for the charring rates with the moisture are very close to the experimental value.

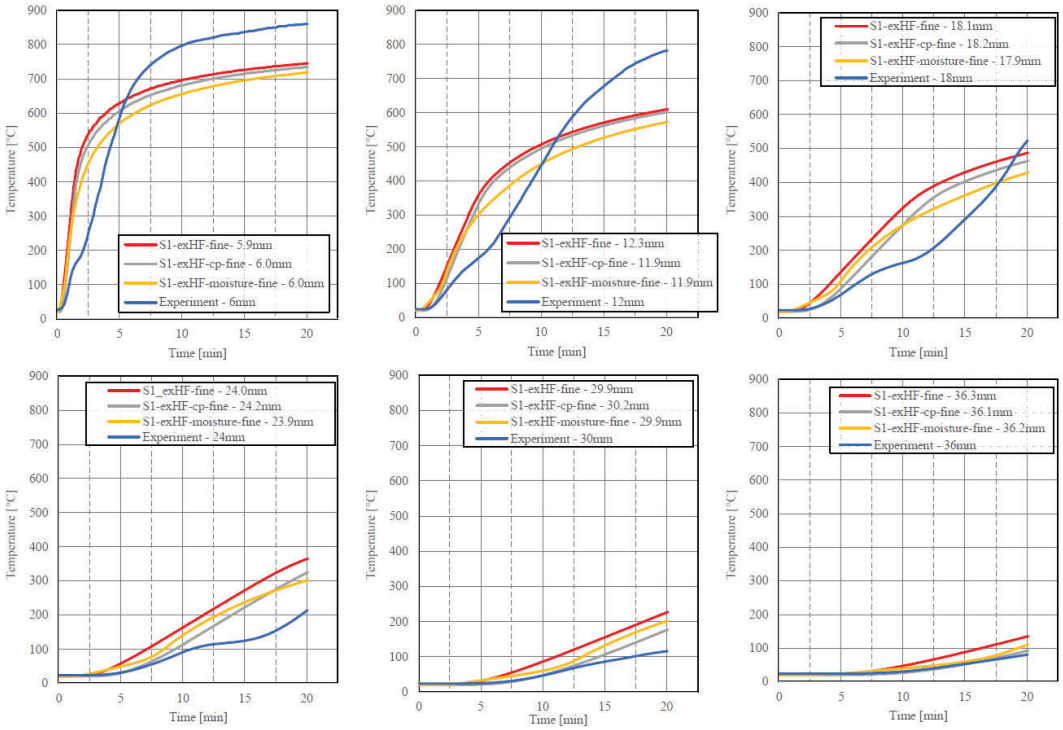

Figure 8: *Comparison of the temperature profile inside the timber specimen for experimental and modelling results at different depths for three specimens: dry, with constant specific heat and moist*

https://doi.org/10.52202/069179-0231

Table 3: *Charring depth and charring rate comparison after 20 minutes*

Parameter	Charring depth (mm)	Charing rate (mm/min)
S1-exHF	26.5	1.33
S1-exHF-moist	23.9	1.20
S1-exHF-cp	24.9	1.25
S2-HP	28.0	1.40
S2-HP-moist	25.4	1.27
Experiment	24.2	1.21

When the moisture is added to the specimen in the simulation, the charring rate decreases. This is because the moisture slows the heat transfer to the solid, resulting in a lower charring depth and rate. The simulation for moist specimen with the external heat flux accurately predicted the charring rate observed in the experiment. The difference is only 0.01 mm/min for the charring rate and 0.3 mm for the charring depth. Moreover, when the heat panel ignites the specimen in the simulation with moisture, the charring depth shows a 4.9% difference from the experimental value and the charring rate has a variation of 0.06 mm/min. Furthermore, it is visible that the simulation with a constant specific heat leads to a lower charring rate compared to the dry specimen and a higher charring rate compared to the moist specimen.

5 CONCLUSIONS

The purpose of the study was to simulate the burning behaviour of a timber specimen using the field model FDS. The simulation coupled the gas and solid phase processes in a fire. The focus was given to predicting the charring depth and the charring rate.

The comparison of the simulation and experimental results revealed a relatively good agreement for the charring rate and surface temperature measurements. The comparison of the temperature profiles inside the timber specimen revealed that the simulation temperatures are generally higher than the experiment temperatures. However, this trend was different close to the exposed timber surface.

The presence of moisture in the pyrolysis model of the timber specimen resulted in lower surface and inlaid temperatures compared to the results with the dry specimen. Further, the moisture influenced the charring rate and it is recommended to include that in the simulation for accurate results. On the other hand, using a constant specific heat instead of a temperature-dependent value also resulted in a slightly smaller charring depth. This shows the dependency of the simulation on the user input data and the importance of selecting accurate inputs for the model. The modified simulations with the constant specific heat showed only a 0.08 mm/min difference in the charring rate compared to the simulation with the temperature-dependent values. Therefore, in the initial simulations it is possible to use a dry specimen with constant specific heat to reduce the computational time while achieving reasonable results for the charring properties. Later, the moisture and temperature-dependent properties can be added to the simulation to achieve a higher level of accuracy.

Even though the simulations showed good agreement with the experiment for the solid phase measurement, there were few variations in the gas phase measurements. Therefore, further research is necessary to improve the simulations and to produce accurate gas phase results. Furthermore, to study the surface regression of the char, a more complex pyrolysis model is needed, including char oxidation.

ACKNOWLEDGEMENT

Authors would like to thank Prof. Dr. Bart Merci and Dr. Andrea Lucherini for the valuable discussions. Furthermore, we are grateful for the support of International Master of Science in Fire Safety Engineering (IMFSE).

REFERENCES

[1] D. Drysdale, An introduction to fire dynamics, 3rd ed. Chichester: Wiley, 2016.

[2] S. Deeny, B. Lane, R. Hadden, and A. Laurence, “Fire Safety Design in Modern Timber Buildings,” *Struct. Eng. J. Inst. Struct. Eng.*, vol. 96, no. 1, pp. 48–53, 2018.

[3] B. Östman, D. Brandon, and H. Frantzich, “Fire safety engineering in timber buildings,” *Fire Saf. J.*, vol. 91, no. May, pp. 11–20, 2017.

[4] J. Schmid and A. Frangi, “Structural timber in compartment fires – the Timber Charring and Heat Storage Model.” *Open Eng.*, vol. 11, no. 1, pp. 435–52, 2021. https://doi.org/10.1515/eng-2021-0043.

[5] C. G. Putynska, A. Law, and J. Torero, “An investigation into the effect of exposed timber on thermal load,” in *Proceedings of the 24th Australasian Conference on the Mec. of Struct. and Mater., ACMSM24*, pp. 939–944, 2016.

[6] J. Schmid, R. Fahrni, A. Frangi, N. Werther, D. Brandon, and A. Just, “Determination of design fires in compartments with combustible structure – modification of existing design equations,” in *Proceedings INTER International Network on Timber Engineering Research 52* , pp. 0–3, 2019.

[7] D. Brandon, C. Dagenais, Fire Safety Challenges of Tall Wood Buildings – Phase 2: Task 5 – Experimental Study of Delamination of Cross Laminated Timber (CLT) in Fire. *National Fire Protection Association*, 2018.

[8] G. De Sanctis, K. Fischer, J. Kohler, M.H. Faber, and M. Fontana, Combining engineering and data-driven approaches: Development of a generic fire risk model facilitating calibration. *Fire Safety Journal*, 70, 23–33, 2014. https://doi.org/10.1016/J.FIRESAF.2014.08.017.

[9] C. Di Blasi, “Modeling and Simulation of Combustion Processes of Charring and Non Charring Solid Fuels,” *Prog. Energy Combust. Sci.*, vol. 19, pp. 71–104, 1993.

[10] S. Sinha, A. Jhalani, M. Ravi, and A. Ray Chaudhury, “Modelling of pyrolysis in wood: a review,” *SESI J.*, vol. 10, no. 1, pp. 41–62, 2000.

[11] L. Shi and M. Y. L. Chew, "A review of thermal properties of timber and char at elevated temperatures," *Indoor Built Environ*., vol. 0, no. 0, pp. 1–16, 2021.
[12] C. Gorska Putynska, "Fire Dynamics in Multi-Scale Timber Compartments," Diss. PHD Thesis, Univ. Queensland., Brisbane, 2019.
[13] B. Moghtaderi, "The state-of-the-art in pyrolysis modelling of lignocellulosic solid fuels," *Fire Mater*., vol. 30, no. 1, pp. 1–34, 2006.
[14] L. Lowden, and T. Hull, Flammability behaviour of wood and a review of the methods for its reduction. *Fire Science Reviews*, 2(1), 4, 2013. https://doi.org/10.1186/2193-0414-2-4.
[15] A. I. Bartlett, R. M. Hadden, and L. A. Bisby, A Review of Factors Affecting the Burning Behaviour of Wood for Application to Tall Timber Construction. *Fire Technology*, 55(1), 1–49, 2019. https://doi.org/10.1007/s10694-018-0787-y.
[16] T. Nyazika, M. Jimenez, F. Samyn, and S. Bourbigot, "Pyrolysis modeling, sensitivity analysis, and optimisation techniques for combustible materials: A review," *J. Fire Sci*., vol. 37, no. 4–6, pp. 377–433, 2019.
[17] N. L. Ryder, J. A. Sutula, C. F., Schemel, A. J. Hamer, and V. Van. Brunt, "Consequence Modeling Using the Fire Dynamics Simulator." *Journal of Hazardous Materials*, vol. 115, no. 1, pp. 149–54, 2004.
[18] K. McGrattan, S. Hostikka, R. McDermott, J. Floyd, C. Weinschenk, and K. Overhold, "Fire Dynamics Simulator User 's Guide (FDS)," *NIST Spec. Publ. 1019*, Sixth Edition, pp. 1-378, 2020.
[19] K. McGrattan, S. Hostikka, R. McDermott, J. Floyd, C. Weinschenk, and K. Overholt, "Fire Dynamics Simulator Technical Reference Guide Volume 1: Mathematical Model," *NIST Spec. Publ. 1019*, Sixth Edition, pp. 1–147, 2015.
[20] A. Rinta-Paavola and S. Hostikka, "A model for the pyrolysis of two Nordic structural timbers," *Fire Mater*., vol. 46, no. 1, pp. 55–68, 2022.
[21] M. Chaos, "Spectral aspects of bench-scale flammability testing: Application to hardwood pyrolysis," *Fire Saf. Sci.*, vol. 11, pp. 165–178, 2014
[22] K. W. Ragland, D. J. Aerts, and A. J. Baker, "Properties of wood for combustion analysis," *Bioresour. Technol.*, vol. 37, no. 2, pp. 161–168, 1991.
[23] M. J. Hurley et al., "SFPE handbook of fire protection engineering, fifth edition," SFPE Handb. Fire Prot. Eng. Fifth Ed., pp. 1–3493, 2016.
[24] J. Faouel, F. Mzali, A. Jemni, and S. Ben Nasrallah, "Thermal conductivity and thermal diffusivity measurements of wood in the three anatomic directions using the transient hot-bridge method," *Spec. Top. Rev. Porous Media*, vol. 3, no. 3, pp. 229–237, 2012.
[25] EN 1995-1-2, Eurocode 5, "Design of timber structures. Part 1-2 General – Structural fire design", European standard, CEN, Brussels, 2004
[26] J. Felder, "Timber Members in Natural Fires - Influencing Parameters in Decay Phase," Master's thesis, ETH Zurich, 2019.
[27] F. Hirzel, "Design Fires for Timber Components - Combustion Behavior, Temperature Profiles and Self-Extinction," Master project thesis, ETH Zurich, 2020

https://doi.org/10.52202/069179-0231